

Cusp-electron production in collisions of open-shell He-like oxygen ions with atomic targets

S. Nanos ^{1,2} N. J. Esponda ³ P.-M. Hillenbrand ^{4,5} A. Biniskos ¹ A. Laoutaris ^{6,2} M. A. Quinto ³ N. Petridis,⁵
E. Menz ^{5,7,8} T. J. M. Zouros ⁶ Th. Stöhlker,^{5,7,8} R. D. Rivarola,^{3,9} J. M. Monti ^{3,9} and E. P. Benis ^{1,*}

¹*Department of Physics, University of Ioannina, GR-45110 Ioannina, Greece*

²*Tandem Accelerator Laboratory, INPP, NCSR Demokritos GR-15310 Agia Paraskevi, Greece*

³*Instituto de Física Rosario (CONICET-UNR), Bulevar 27 de Febrero 210 bis, 2000 Rosario, Argentina*

⁴*I. Physikalisches Institut, Justus-Liebig-Universität, 35392 Giessen, Germany*

⁵*GSI Helmholtzzentrum für Schwerionenforschung, 64291 Darmstadt, Germany*

⁶*Department of Physics, University of Crete, GR-70013 Heraklion, Greece*

⁷*Institut für Optik und Quantenelektronik, Friedrich-Schiller-Universität, 07743 Jena, Germany*

⁸*Helmholtz-Institut Jena, 07743 Jena, Germany*

⁹*Laboratorio de Colisiones Atómicas, FCEIA, IFIR, Universidad Nacional de Rosario, Avenida Pellegrini 250, Rosario 2000, Argentina*



(Received 29 March 2023; accepted 30 May 2023; published 15 June 2023)

We report on double differential cross sections of cusp electrons obtained in MeV/u collisions of open-shell He-like oxygen ions with helium. We use zero-degree electron spectroscopy and our double measurement technique, involving $O^{6+}(1s^2)$ ground-state and $O^{6+}(1s^2, 1s2s)$ mixed-state beams, to extract the cusp contribution from only the excited $O^{6+}(1s2s)$ beam. Theoretical calculations based on the continuum distorted wave eikonal initial state are in very good agreement with the measurements. The roles of the processes of electron capture to the continuum, electron loss to the continuum, and electron loss to the continuum with simultaneous target ionization, which contribute to the cusp peak, are discussed in detail.

DOI: [10.1103/PhysRevA.107.062815](https://doi.org/10.1103/PhysRevA.107.062815)

I. INTRODUCTION

Fast ion-atom collisions involving unpaired electrons have proven to be a powerful tool for studying subtle dynamic aspects of fundamental processes. Experimental results from such systems not only submit theoretical collision approximations and models to stringent tests but also pave the way to the development of more advanced theories. Thus, effects originating from the dynamics of spin symmetries, hidden population mechanisms, electronic correlation [1–3], and the stopping power in media [4] have been investigated. Research fields that use atomic collision data, such as astrophysical and laboratory plasmas [5–8], greatly benefit from such advancements.

Collisions with pre-excited ions delivered by various types of accelerators are often used for studies on fundamental collision processes [9–14]. However, so far the processes of target electron capture to the continuum (ECC) [15] and its counterpart, projectile electron loss to the continuum (ELC) [16], have not been examined in collisions with pre-excited ions. The dynamics of these processes rely on the two-center effects of the combined long-range Coulombic fields of the projectile and the target [17]. Both processes result in a characteristic cusp-shaped peak in the double differential cross section (DDCS) electron spectra observed around zero degrees with respect to the projectile beam, with emission velocities close to the projectile velocity.

The cusp-shaped peak has been successfully described by continuum distorted wave (CDW) and continuum distorted wave-eikonal initial state (CDW-EIS) theories [18]. During the past decades, distorted theories have been thoroughly developed to explain interesting experimental results on cusp electrons such as the production of cusp-shaped peaks from neutral projectiles [19,20] and the role of the target subshells in collisions with multielectronic targets [21,22]. In addition, distorted wave theories have also been developed for near-relativistic collisions involving heavy-ion projectiles. Thus, the dynamics of ELC [23,24], ECC [25], and radiative ECC [26,27] were detailed for this collision region.

Here, we report on a combined experimental and theoretical study of cusp electrons produced in 24-MeV collisions of open-shell $O^{6+}(1s2s)$ projectiles with He targets. The experimental cusp DDCS electron spectra were obtained by applying our double measurement technique, involving a measurement with a mixed-state $O^{6+}(1s^2, 1s2s)$ and a measurement with a ground state $O^{6+}(1s^2)$ beam. Theoretical cusp DDCS results, obtained within the CDW-EIS framework, are compared to the measurements, showing an overall good agreement. Details involving the contributions of the ECC and ELC processes from the different ion cores are discussed.

II. EXPERIMENT

To expose the most sensitive characteristic of cusp electrons we performed measurements at zero degrees with respect to the ion beam trajectory, applying the technique of zero-degree Auger projectile spectroscopy (ZAPS) [28]. The

*mbenis@uoi.gr

experiments were conducted at the NCSR “Demokritos” 5.5-MV tandem accelerator laboratory, utilizing our ZAPS setup at the APAPES installation [29]. This setup has been described in detail elsewhere [30,31] and only a short description of its operation is given here.

The heart of our ZAPS setup is a hemispherical spectrograph, which consists of an electrostatic single-stage hemispherical deflector analyzer (HDA) equipped with a four-element injection lens and a two-dimensional position-sensitive detector (PSD). The projectile beam interacts with the gas target, formed by a doubly differentially pumped gas cell. The electrons emitted within a polar angle $\theta_{\max} = 0.4^\circ$ with respect to the projectile velocity are focused by the spectrograph entry lens, energetically analyzed by the HDA, and imaged onto the PSD along the dispersion axis [32]. The ion beam passes through the spectrograph to be collected in a Faraday cup for normalization purposes. The setup is magnetically shielded by using double μ -metal shielding.

The measured electron DDCS is determined according to the following formula [28]:

$$\text{DDCS}_j \equiv \frac{d^2\sigma_j}{d\Omega dE_j} = \frac{N_j^e}{N_I L_{\text{eff}} n \Delta\Omega \Delta E_j T \eta}, \quad (1)$$

where N_j^e is the number of electrons detected in channel j , L_{eff} is the effective length of the target gas cell, N_I is the number of ions collected in the Faraday cup, n is the target gas density, $\Delta\Omega$ is the solid angle determined by the entry aperture of the lens and the distance of the center of the target gas cell from it, ΔE_j is the energy step per channel in the spectrum, and T is the analyzer transmission determined by the three 90% transmission meshes. The overall efficiency η was obtained by performing auxiliary *in situ* measurements of elastically scattered (binary encounter) electrons from bare ion beams, resulting in an overall efficiency of $\eta = (50 \pm 5)\%$ [33].

The measurement of the cusp continuum does not necessitate high resolution in energy measurements. Thus, we operated the spectrograph in the low-resolution mode. Under these conditions, an electron spectrum covers an energy range of about 20% of the tuning energy. To cover the entire cusp peak, several overlapping energy windows were recorded at the appropriate tuning energies and then pieced together [22].

Background spectra, corresponding to measurements without target gas, were also recorded and subtracted from the spectra with the gas target. Then, the resulting spectra were energy calibrated according to known energy vs channel calibration formulas, and the DDCSs were obtained according to Eq. (1). Single-collision conditions were ensured by properly adjusting the target gas pressure. An overall absolute uncertainty of about 15% is inherent in all our DDCS measurements.

The dynamics of the cusp-scattered electrons resulting from open-shell He-like atoms were experimentally investigated by applying our double measurement technique [34]. In this approach, in a few MeV/u collisions of He-like ions with He or H_2 targets, the electron spectrum is measured twice, exploiting He-like beams with appreciably different $(1s^2, 1s2s)$ configuration fractional content. He-like ion beams produced in tandem Van de Graaff accelerators are in general delivered in a mixture of $1s^2$ ground and $1s2s$ configurations [35]. In

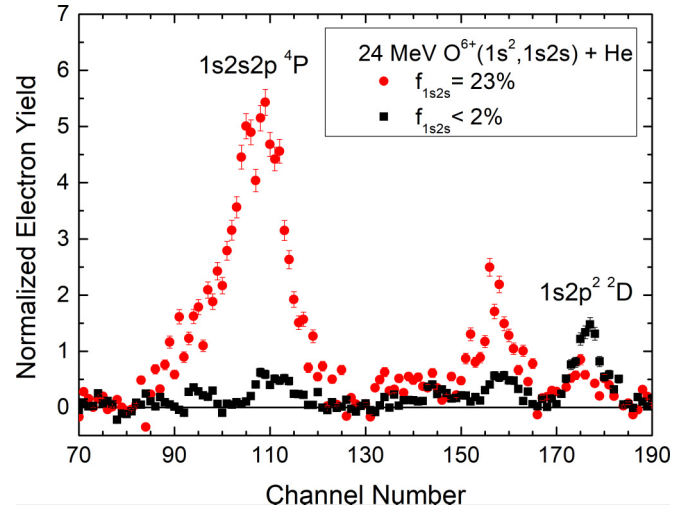


FIG. 1. KLL Auger spectra measured at zero degrees with respect to the projectile velocity for collisions of 24-MeV $\text{O}^{6+}(1s^2, 1s2s)$ with He gas targets. The red solid circles correspond to a mixed-state beam with a high-value fraction, $f_{1s2s} = (23 \pm 4)\%$, while the black solid squares correspond to a very low-value fraction, $f_{1s2s} < 2\%$, i.e., to a practically pure ground-state beam.

more detail, the $1s2s$ configuration is delivered in the $1s2s\ ^1S$ and $1s2s\ ^3S$ states. However, we do not examine them separately here, since, as we show below, the $1s2s\ ^1S$ component does not survive to the target area due to its small lifetime. The fractions of the mixture depend on the stripping medium (thin foil or gas) for up-charging the ion beam, as well as the stripping energy. As a consequence, the He-like beam content can be controlled, resulting in a high or low $1s2s$ fraction when thin foils or gases are used for the up-charging, respectively. Moreover, in the case of gases, an almost pure ground state may be delivered for adequately low stripping energies [36].

In Fig. 1, we present an example of the double measurement technique, necessary for the reported cusp study, where the $1s2s2l$ KLL Auger spectra obtained in collisions of 24-MeV O^{6+} beams with He targets are measured for two $\text{O}^{6+}(1s^2, 1s2s)$ beams with notably different $(1s^2, 1s2s)$ configuration fractional content. For this collision energy, the $1s2s2p\ ^4P$ state results from the $1s2s\ ^3S$ state via single-electron capture, while the $1s2p^2\ ^2D$ state results from the $1s^2\ ^1S$ state via transfer-excitation [37]. Under these conditions, single differential cross sections can be obtained for all the KLL states produced from He-like mixed-state beams by applying our double measurement technique [34,37]. In addition, the value of the fractions of the beam components, necessary for the current cusp study, are also obtained as [34,38]

$$f_{1s2s\ ^3S}^i = \frac{Y_i[{}^4P] (Y_2[{}^2D] - Y_1[{}^2D])}{Y_2[{}^2D]Y_1[{}^4P] - Y_1[{}^2D]Y_2[{}^4P]}, \quad i = 1, 2, \quad (2)$$

where Y_i is the normalized yield of the $({}^{2S+1})L$ Auger states, with $i = 1$ and 2 corresponding to each of the two measurements having different fractions.

The fraction f_{1s2s} , necessary for our cusp studies, is obtained from the determination of the fraction $f_{1s2s\ ^3S}$, assuming

that the $1s2s\ ^1S$ and $1s2s\ ^3S$ states are statistically produced with a ratio of 1/3, and considering their survival percentage to the experimental area according to their lifetimes. The lifetimes of $1s2s\ ^1S$ and $1s2s\ ^3S$ states are 4.3×10^{-7} and 9.6×10^{-4} s, respectively [35]. By taking into account that the velocity of the 24-MeV O^{6+} beam is 1.7×10^7 m/s, and the distance between the production area at the accelerator tank and the target area is 26.4 m, we conclude that the initial population of the $1s2s\ ^3S$ state remains unaffected. However, for the $1s2s\ ^1S$ state, its initial population is reduced by about a factor of 10, corresponding to the 1/30 of the population of the $1s2s\ ^3S$ state, and thus can be safely neglected. Therefore, for these experimental conditions, we may obtain the f_{1s2s} fraction from Eq. (2), since $f_{1s2s} \simeq f_{1s2s\ ^3S}$. In this way, for the spectra shown in Fig. 1, the high and low f_{1s2s} fractions were obtained as $f_{1s2s} = (23 \pm 4)\%$ and $f_{1s2s} < 2\%$, respectively. The latter is well within the experimental uncertainty, and thus we may well consider this case as a pure ground-state beam.

III. THEORY

The experimental DDCSs are accompanied by corresponding theoretical calculations based on the CDW-EIS framework. CDW theories have been recently reviewed in Ref. [39]. Briefly, CDW theories are perturbative approaches where a target bound-electron wave function is distorted by a projectile continuum factor, and then, in the case of ionization, the ejected electron is described in the continuum of both target and projectile. For this reason, they are also referred to as two-center theories. In addition, we note that an independent-electron approach was considered.

The extension of these CDW theories for electron emission in collision systems involving dressed projectiles has been addressed in Ref. [40]. In this case, the projectile potential is considered as the sum of a long-range Coulombic potential and a screened short-range potential. The screening function that determines the short-range interaction depends on parameters already tabulated for a wide variety of ground-state ions [41]. However, for the $O^{6+}(1s2s)$ excited state examined here, there are no parameters tabulated elsewhere, so we have calculated the corresponding potential. The projectile potential is then determined by the interaction of the target active electron with the projectile nucleus and also its interaction with the projectile electrons averaged over their electronic distribution. As a final step, the total potential, resulting from the sum of the above electronic repulsion and the nuclear attraction, is rewritten in the form of a long-range term, with an asymptotic net charge, and a short-range screened potential.

The excited state $1s2s$ projectile orbitals were obtained through Hartree-Fock wave functions proposed in Ref. [42]. This method can go beyond the determination of ground states reported in Ref. [43] and allows for representing the lower excited states of atoms and ions, having up to 18 electrons, in an analytical form with an error close to the numerical solution [42]. Then, each shell is described in terms of Slater orbitals.

In addition, for dressed projectiles within the CDW-EIS framework, a dynamic effective charge that was recently proposed in Ref. [20] for the final-channel projectile continuum

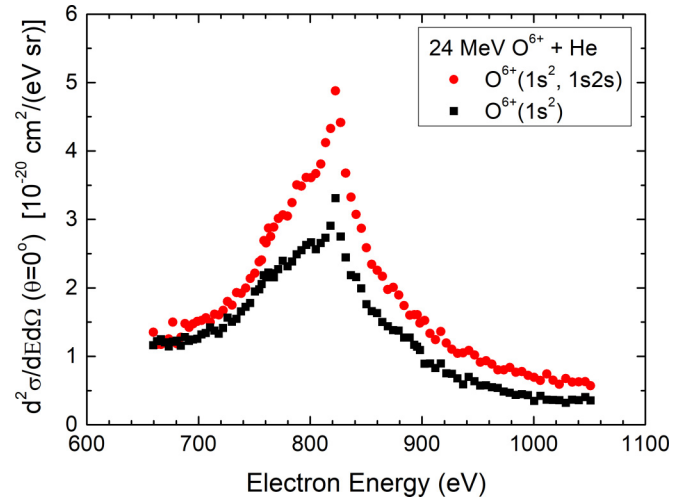


FIG. 2. Zero-degree DDCS of cusp electrons measured in collisions of 24-MeV O^{6+} with He gas targets. Red solid circles: Mixed-state $O^{6+}(1s^2, 1s2s)$ beam with $f_{1s2s} = 23\%$. Black solid squares: Ground-state $O^{6+}(1s^2)$ beam.

factor is also considered here. By its use we may account for collision dynamics where the projectile nuclear charge is not fully screened by its bounded electrons [20,33], as is the present case. The dynamic effective charge is defined using the projectile form factor, and thus, since it depends on its electronic configuration, it differs for the ground and excited states. Thus, the excited projectiles are less screened or, in other words, their potential is spatially more spread out.

According to the above considerations we have calculated the target ionization by ground-state or excited-state projectile impact, particularly, the ECC process. Then, for the ELC process, we reverse the collision system and then transform the DDCS from the projectile reference frame to the laboratory one [18]. Finally, the simultaneous ionization of both collision partners is estimated by means of their single-ionization DDCSs and total cross sections, as done in Ref. [44].

IV. RESULTS AND DISCUSSION

In Fig. 2 we present the DDCS cusp measurements obtained for collisions of He-like O^{6+} beams with He targets, which correspond to those performed for the KLL Auger spectra shown in Fig. 1. We obtained the cusp peak for the $O^{6+}(1s^2, 1s2s)$ mixed-state beam with a fraction of $f_{1s2s} = (23 \pm 4)\%$ and for the almost pure ground-state beam $O^{6+}(1s^2)$. The maximum of the cusp peak corresponds to the reduced projectile energy t_p determined as $t_p = \frac{m}{M_p} E_p$ [28], where E_p and M_p are the kinetic energy and the mass of the projectile, respectively, while m is the electron mass. The difference in the magnitude as well as the shape of the two corresponding cusp peaks is evident and is discussed below along with the corresponding theoretical results.

The contributions of the ECC and ELC processes to the DDCS cusp peak, obtained from CDW-EIS calculations for collisions of 24-MeV $O^{6+}(1s^2)$ and 24-MeV $O^{6+}(1s2s)$ with

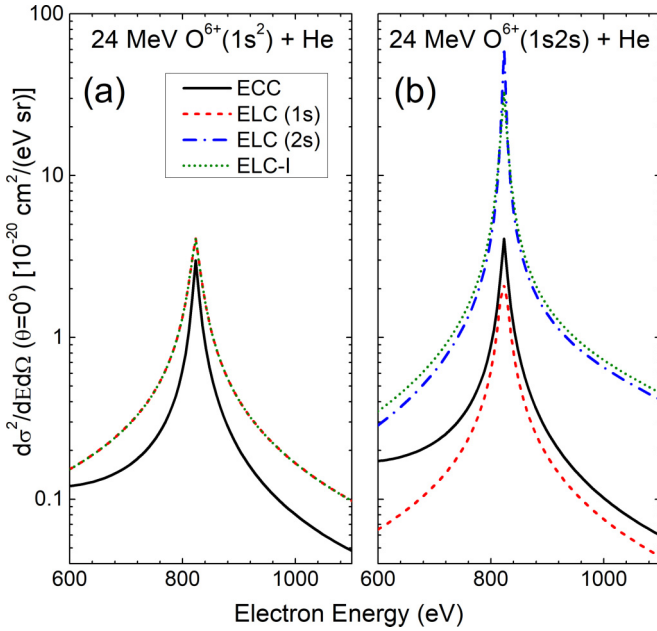


FIG. 3. CDW-EIS calculations for zero-degree DDCCS of cusp electrons for collisions of (a) 24-MeV $O^{6+}(1s^2)$ and (b) 24-MeV $O^{6+}(1s2s)$ with He gas targets. Black solid lines: ECC contribution. Red short dashed line: ELC from the $1s$ electron. Blue dash-dotted line: ELC from the $2s$ electron. Green short-dotted line: Total ELC with simultaneous He target single ionization.

He targets, are shown in Fig. 3. There, it is clearly seen that the ELC cross section from the $2s$ electron [ELC($2s$)] is larger by almost an order of magnitude compared to the ELC cross section for the $1s$ electron [ELC($1s$)] or the ECC cross section for both configurations. In addition, the ELC from both $1s$ and $2s$ electrons with the simultaneous single ionization of the He target (ELC-I) is also included in the CDW-EIS calculations, showing a contribution almost equal to that of the ELC($1s$) and ELC($2s$) cross sections for the ground and excited projectile cases, respectively.

It is interesting to note that the ELC($1s$) cross section for the $O^{6+}(1s2s)$ configuration is smaller compared to that of the $O^{6+}(1s^2)$ configuration, even though the latter accounts for two electrons and thus has to be divided by 2 for a fair comparison. This is attributed to the smaller screening for the $1s$ electron of the $O^{6+}(1s2s)$ configuration, which leads to a different binding energy, as detailed above. Moreover, the ECC process depends, although in this case not strongly, on the projectile electronic configuration through the projectile potential. However, it is worth mentioning that the ECC cross section for the $O^{6+}(1s2s)$ configuration appears to be larger than that of the $O^{6+}(1s^2)$ one and more asymmetric. This might be related to the larger volume covered by the electrons of the $O^{6+}(1s2s)$ configuration that favors capture. A similar cusp enhancement due to metastable projectiles has been reported in Ref. [45]. Thus, the measured higher DDCCS magnitude for the mixed-state beam is primarily due to the contribution of the larger ELC($2s$) cross section. The enhanced contribution of the ELC process is also qualitatively evident from the shape of the low-energy cusp wing. The ECC

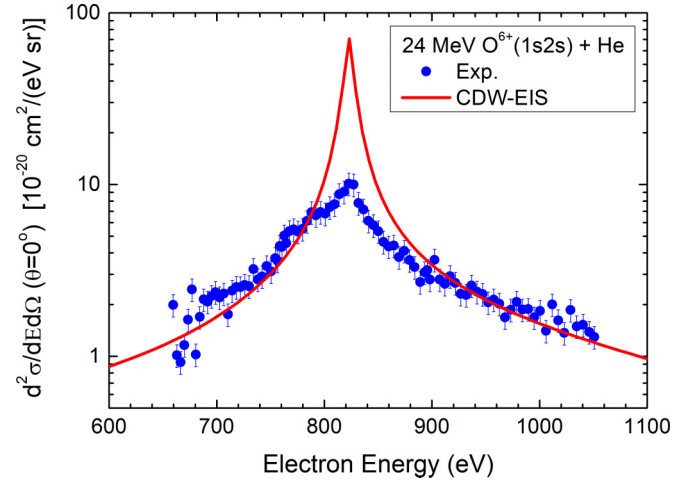


FIG. 4. Zero-degree DDCCS of cusp electrons for collisions of 24-MeV $O^{6+}(1s2s)$ with He gas targets. Blue solid circles: Experimental data obtained from the double measurement cusp data shown in Fig. 2. Red line: Calculations based on the CDW-EIS theory.

process has a much more asymmetric distribution than the ELC process [18]. Thus, for the case of the ground state, where the ECC process is pronounced, the asymmetry of the cusp peak is larger compared to the asymmetry of the mixed-state beam, where the ELC($2s$) cross section is predominant.

In the double measurement technique and in the case where one of the measurements corresponds to a pure $1s^2$ ground-state beam, then the electron DDCCS spectra, corresponding only to the open-shell $1s2s$ configuration, can be straightforwardly obtained according to the following formula:

$$\frac{d^2\sigma[1s2s]}{d\Omega dE} = \frac{\frac{d^2\sigma[1s^2, 1s2s]}{d\Omega dE} - (1 - f_{1s2s}) \frac{d^2\sigma[1s^2]}{d\Omega dE}}{f_{1s2s}}. \quad (3)$$

In this study, special care was taken in order to satisfy these conditions as evident from the DDCCS cusp spectra presented in Fig. 2. Thus, by applying Eq. (3) to the data of Fig. 2, we obtained the DDCCS cusp spectra corresponding only to the open-shell $O^{6+}(1s2s)$ configuration. In Fig. 4 we present the experimental result along with the calculations of the CDW-EIS theory, already presented in Fig. 3(b) for each process contribution separately. Although the cusp calculations were averaged over the experimental polar angle θ , energy convolution with the experimental resolution was not considered, since the latter is of the order of the energy step of the calculations, i.e., $\Delta E/E \simeq 1\%$. The experimental uncertainties are primarily due to the uncertainty of the determination of the f_{1s2s} fraction.

It is evident that CDW-EIS calculations reproduce adequately the wings of the cusp peak. The energy position of the peak is given by a mathematical pole and, therefore, its height is subjected to variations depending on the integration process. The very nice agreement at the wings of the cusp peak strongly indicates that well-established and sophisticated collision theories such as CDW-EIS are further advanced when tested against nontrivial collision systems. Thus, in our case, the introduction of appropriate projectile screened potentials,

as well as the high-quality projectile wave functions for the $1s2s$ excited state, resulted in a very good agreement with the cusp data, thus justifying these advancements. In addition, these improvements in the CDW-EIS framework of collisions with dressed projectiles exposed some interesting features about the role of the ECC and ELC processes in the production of cusp electrons, as detailed above.

V. CONCLUSIONS

In conclusion, we studied both experimentally and theoretically the formation of cusp electron peaks resulting from MeV/u collisions of open-shell He-like oxygen ions $O^{6+}(1s2s)$ with helium. The experimental data were obtained after applying our double measurement technique, involving $O^{6+}(1s^2)$ ground-state and $O^{6+}(1s^2, 1s2s)$ mixed-state beams. CDW-EIS theoretical calculations for dressed ions, modified

to include appropriate potential screening and excited wave functions, show a very good agreement with the DDCS measurements. Moreover, CDW-EIS calculations expose the roles of the ECC and ELC processes and their contributions to the cusp peak.

ACKNOWLEDGMENTS

S.N. acknowledges financial support by the program “Strengthening and Supporting the Operation of Developmental, Research, and Educational Activities of the University of Ioannina.” S.N., P.-M.H., A.B., A.L., N.P., E.M., T.S., and E.P.B. acknowledge support by the project “IKYDA2020” of the IKY-DAAD Greek-German Collaboration. N.J.E., M.A.Q., R.D.R., and J.M.M. acknowledge financial support from Consejo Nacional de Investigaciones Científicas y Técnicas of Argentina, Project No. PIP 2021-3245.

-
- [1] I. Madesis, A. Laoutaris, T. J. M. Zouros, E. P. Benis, J. W. Gao, and A. Dubois, Pauli Shielding and Breakdown of Spin Statistics in Multielectron Multi-Open-Shell Dynamical Atomic Systems, *Phys. Rev. Lett.* **124**, 113401 (2020), and Supplemental Material.
- [2] A. Laoutaris, S. Nanos, I. Madesis, S. Passalidis, E. P. Benis, A. Dubois, and T. J. M. Zouros, Coherent treatment of transfer-excitation processes in swift ion-atom collisions, *Phys. Rev. A* **106**, 022810 (2022).
- [3] I. Bray, D. V. Fursa, A. S. Kadyrov, A. Müller, A. Borovik, and S. Schippers, Spin asymmetry in electron-impact ionization, *Phys. Rev. A* **100**, 012707 (2019).
- [4] Y. T. Zhao, Y. N. Zhang, R. Cheng, B. He, C. L. Liu, X. M. Zhou, Y. Lei, Y. Y. Wang, J. R. Ren, X. Wang, Y. H. Chen, G. Q. Xiao, S. M. Savin, R. Gavrilin, A. A. Golubev, and D. H. H. Hoffmann, Benchmark Experiment to Prove the Role of Projectile Excited States Upon the Ion Stopping in Plasmas, *Phys. Rev. Lett.* **126**, 115001 (2021).
- [5] P. Beiersdorfer, J. H. Scofield, and A. L. Osterheld, X-Ray-Line Diagnostic of Magnetic Field Strength for High-Temperature Plasmas, *Phys. Rev. Lett.* **90**, 235003 (2003).
- [6] A. K. Pradhan and S. N. Nahar, *Atomic Astrophysics and Spectroscopy* (Cambridge University, Cambridge, England, 2011).
- [7] V. P. Shevelko and H. Tawara (eds.), *Atomic Processes in Basic and Applied Physics* (Springer, Berlin, 2012).
- [8] R. Betti and O. A. Hurricane, Inertial-confinement fusion with lasers, *Nat. Phys.* **12**, 435 (2016).
- [9] R. Ben-shlomi, R. Vexiau, Z. Meir, T. Sikorsky, N. Akerman, M. Pinkas, O. Dulieu, and R. Ozeri, Direct observation of ultracold atom-ion excitation exchange, *Phys. Rev. A* **102**, 031301(R) (2020).
- [10] A. Gumberidze, D. Thorn, A. Surzhykov, C. Fontes, H. Bana^Å, D. Beyer, R. Chen, W. Grisenti, S. Hagmann, R. Hess, P.-M. Hillenbrand, P. Indelicato, C. Kozhuharov, M. Lestinsky, R. M^ärtin, N. Petridis, R. Popov, R. Schuch, U. Spillmann, S. Tashenov *et al.*, Angular distribution of characteristic radiation following the excitation of He-like uranium in relativistic collisions, *Atoms* **9**, 20 (2021).
- [11] S. Schippers, S. Stock, T. Buhr, A. Perry-Sassmannshausen, S. Reinwardt, M. Martins, A. Müller, and S. Fritzsche, Near K-edge photoionization and photoabsorption of singly, doubly, and triply charged silicon ions, *Astrophys. J.* **931**, 100 (2022).
- [12] Z. Huang, S. Wang, W. Wen, H. Wang, W. Ma, C. Chen, C. Zhang, D. Chen, H. Huang, and L. Shao, Absolute dielectronic recombination rate coefficients of highly charged ions at the storage ring CSRm and CSRe, *Chi. Phys. B* (2023), doi:10.1088/1674-1056/acbc69.
- [13] B. C. de Miranda, C. Romanzin, S. Chefdeville, V. Vuitton, J. Žabka, M. Poláček, and C. Alcaraz, Reactions of state-selected atomic oxygen ions $O^+(^4S, ^2D, ^2P)$ with methane, *J. Phys. Chem. A* **119**, 6082 (2015).
- [14] R. Hubele, A. LaForge, M. Schulz, J. Goullon, X. Wang, B. Najjari, N. Ferreira, M. Grieser, V. L. B. de Jesus, R. Moshhammer, K. Schneider, A. B. Voitkiv, and D. Fischer, Polarization and Interference Effects in Ionization of Li by Ion Impact, *Phys. Rev. Lett.* **110**, 133201 (2013).
- [15] G. B. Crooks and M. E. Rudd, Experimental Evidence for the Mechanism of Charge Transfer into Continuum States, *Phys. Rev. Lett.* **25**, 1599 (1970).
- [16] D. Burch, H. Wieman, and W. B. Ingalls, Electron Loss in High-Energy Oxygen-Ion Collisions, *Phys. Rev. Lett.* **30**, 823 (1973).
- [17] P. D. Fainstein, V. H. Ponce, and R. D. Rivarola, Two-centre effects in ionization by ion impact, *J. Phys. B: At., Mol. Opt. Phys.* **24**, 3091 (1991).
- [18] N. Stolterfoht, R. D. DuBois, and R. D. Rivarola, *Electron Emission in Heavy Ion-Atom Collisions*, Springer Series on Atomic, Optical, and Plasma Physics, Vol. 20 (Springer, Berlin, 1997).
- [19] L. Sarkadi, J. Pálinkás, A. Kövér, D. Berényi, and T. Vajnai, Observation of Electron Capture into Continuum States of Neutral Atoms, *Phys. Rev. Lett.* **62**, 527 (1989).
- [20] N. J. Esponda, M. A. Quinto, R. D. Rivarola, and J. M. Monti, Dynamic screening and two-center effects in neutral and partially dressed ion-atom collisions, *Phys. Rev. A* **105**, 032817 (2022).
- [21] M. Rodbro and F. Andersen, Charge transfer to the continuum for 15 to 1500 keV H^+ in He, Ne, Ar and H_2 gases under single-collision conditions, *J. Phys. B: At. Mol. Phys.* **12**, 2883 (1979).
- [22] S. Nanos, M. A. Quinto, I. Madesis, A. Laoutaris, T. J. M. Zouros, R. D. Rivarola, J. M. Monti, and E. P. Benis, Subshell

- contributions to electron capture into the continuum in MeV/u collisions of deuterons with multielectron targets, *Phys. Rev. A* **105**, 022806 (2022).
- [23] P.-M. Hillenbrand, S. Hagmann, J. M. Monti, R. D. Rivarola, K.-H. Blumenhagen, C. Brandau, W. Chen, R. D. DuBois, A. Gumberidze, D. L. Guo, M. Lestinsky, Y. A. Litvinov, A. Müller, S. Schippers, U. Spillmann, S. Trotsenko, G. Weber, and T. Stöhlker, Strong asymmetry of the electron-loss-to-continuum cusp of multielectron U^{28+} projectiles in near-relativistic collisions with gaseous targets, *Phys. Rev. A* **93**, 042709 (2016).
- [24] P.-M. Hillenbrand, K. N. Lyashchenko, S. Hagmann, O. Y. Andreev, D. Banaś, E. P. Benis, A. I. Bondarev, C. Brandau, E. De Filippo, O. Forstner, J. Glorius, R. E. Grisenti, A. Gumberidze, D. L. Guo, M. O. Herdrich, M. Lestinsky, Y. A. Litvinov, E. V. Pagano, N. Petridis, M. S. Sanjari *et al.*, Electron-loss-to-continuum cusp in collisions of U^{89+} with N_2 and Xe, *Phys. Rev. A* **104**, 012809 (2021).
- [25] P.-M. Hillenbrand, S. Hagmann, D. H. Jakubassa-Amundsen, J. M. Monti, D. Banaś, K.-H. Blumenhagen, C. Brandau, W. Chen, P. D. Fainstein, E. De Filippo, A. Gumberidze, D. L. Guo, M. Lestinsky, Y. A. Litvinov, A. Müller, R. D. Rivarola, H. Rothard, S. Schippers, M. S. Schöffler, U. Spillmann *et al.*, Electron-capture-to-continuum cusp in $U^{88+} + N_2$ collisions, *Phys. Rev. A* **91**, 022705 (2015).
- [26] P.-M. Hillenbrand, S. Hagmann, D. Atanasov, D. Banaś, K.-H. Blumenhagen, C. Brandau, W. Chen, E. De Filippo, A. Gumberidze, D. L. Guo, D. H. Jakubassa-Amundsen, O. Kovtun, C. Kozhuharov, M. Lestinsky, Y. A. Litvinov, A. Müller, R. A. Müller, H. Rothard, S. Schippers, M. S. Schöffler *et al.*, Radiative-electron-capture-to-continuum cusp in $U^{88+} + N_2$ collisions and the high-energy endpoint of electron-nucleus bremsstrahlung, *Phys. Rev. A* **90**, 022707 (2014).
- [27] P.-M. Hillenbrand, S. Hagmann, M. E. Groshev, D. Banaś, E. P. Benis, C. Brandau, E. De Filippo, O. Forstner, J. Glorius, R. E. Grisenti, A. Gumberidze, D. L. Guo, B. Hai, M. O. Herdrich, M. Lestinsky, Y. A. Litvinov, E. V. Pagano, N. Petridis, M. S. Sanjari, D. Schury *et al.*, Radiative electron capture to the continuum in $U^{89+} + N_2$ collisions: Experiment and theory, *Phys. Rev. A* **101**, 022708 (2020).
- [28] T. J. M. Zouros and D. H. Lee, Zero degree Auger electron spectroscopy of projectile ions, in *Accelerator-Based Atomic Physics: Techniques and Applications*, edited by S. M. Shafroth and J. C. Austin (American Institute of Physics, Woodbury, NY, 1997), Chap. 13, pp. 426–479.
- [29] S. Harissopoulos, M. Andrianis, M. Axiotis, A. Lagoyannis, A. G. Karydas, Z. Kotsina, A. Laoutaris, G. Apostolopoulos, A. Theodorou, T. J. M. Zouros, I. Madesis, and E. P. Benis, The Tandem Accelerator Laboratory of NCSR Demokritos: Current status and perspectives, *Eur. Phys. J. Plus* **136**, 617 (2021).
- [30] I. Madesis, A. Dimitriou, A. Laoutaris, A. Lagoyannis, M. Axiotis, T. Mertzimekis, M. Andrianis, S. Harissopoulos, E. P. Benis, B. Sulik, I. Valastyán, and T. J. M. Zouros, Atomic physics with accelerators: Projectile electron spectroscopy (APAPES), *J. Phys.: Conf. Ser.* **583**, 012014 (2015).
- [31] I. Madesis, A. Laoutaris, T. J. M. Zouros, S. Nanos, and E. P. Benis, Projectile electron spectroscopy and new answers to old questions: Latest results at the new atomic physics beamline in Demokritos, Athens, in *State-of-the-Art Reviews on Energetic Ion-Atom and Ion-Molecule Collisions*, Interdisciplinary Research on Particle Collisions and Quantitative Spectroscopy, Vol. 2, edited by D. Belkić, I. Bray, and A. Kadyrov (World Scientific, Singapore, 2019), Chap. 1, pp. 1–31.
- [32] T. J. M. Zouros and E. P. Benis, The hemispherical deflector analyser revisited. I. Motion in the ideal $1/r$ potential, generalized entry conditions, Kepler orbits and spectrometer basic equation, *J. Electron Spectrosc. Relat. Phenom.* **125**, 221 (2002).
- [33] N. J. Esponda, S. Nanos, M. A. Quinto, T. J. M. Zouros, R. D. Rivarola, E. P. Benis, and J. M. Monti, Binary encounter electrons in fast dressed-ion- H_2 collisions: Distorted wave theories and experiment, *Atoms* **11**, 17 (2023).
- [34] E. P. Benis, S. Doukas, and T. J. M. Zouros, Evidence for the non-statistical population of the $1s2s2p^4P$ metastable state by electron capture in 4 MeV collisions of $B^{3+}(1s2s^3S)$ with H_2 targets, *Nucl. Instrum. Methods Phys. Res., Sect. B* **369**, 83 (2016).
- [35] E. P. Benis, I. Madesis, A. Laoutaris, S. Nanos, and T. J. M. Zouros, Mixed-state ionic beams: An effective tool for collision dynamics investigations, *Atoms* **6**, 66 (2018).
- [36] M. Zamkov, H. Aliabadi, E. P. Benis, P. Richard, H. Tawara, and T. J. M. Zouros, Energy dependence of the metastable fraction in $B^{3+}(1s^2\ ^1S, 1s2s\ ^3S)$ beams produced in collisions with thin-foil and gas targets, *Phys. Rev. A* **64**, 052702 (2001).
- [37] I. Madesis, A. Laoutaris, S. Nanos, S. Passalidis, A. Dubois, T. J. M. Zouros, and E. P. Benis, State-resolved differential cross sections of single electron capture in swift collisions of $C^{4+}(1s2s^3S)$ ions with gas targets, *Phys. Rev. A* **105**, 062810 (2022).
- [38] E. P. Benis, M. Zamkov, P. Richard, and T. J. M. Zouros, Technique for the determination of the $1s2s^3S$ metastable fraction in two-electron ion beams, *Phys. Rev. A* **65**, 064701 (2002).
- [39] R. D. Rivarola, O. A. Fojón, M. Ciappina, and D. Crothers, Continuum distorted wave and Wannier methods, in *Springer Handbook of Atomic, Molecular, and Optical Physics*, edited by G. W. F. Drake (Springer, Cham, 2023), pp. 813–828.
- [40] J. M. Monti, R. D. Rivarola, and P. D. Fainstein, Distorted wave theories for dressed-ion-atom collisions with GSZ projectile potentials, *J. Phys. B: At., Mol. Opt. Phys.* **44**, 195206 (2011).
- [41] P. P. Szydlik and A. E. S. Green, Independent-particle-model potentials for ions and neutral atoms with $Z \leq 18$, *Phys. Rev. A* **9**, 1885 (1974).
- [42] N. V. Novikov, New method of the approximation of Hartree-Fock wave functions, *Int. J. Math. Comp. Sci.* **1**, 55 (2015).
- [43] B. Cleff and W. Mehlhorn, On the angular distribution of Auger electrons following impact ionization, *J. Phys. B: At. Mol. Phys.* **7**, 593 (1974).
- [44] D. Fregenal, J. M. Monti, J. Fiol, P. D. Fainstein, R. D. Rivarola, G. Bernardi, and S. Suárez, Experimental and theoretical results on electron emission in collisions between He targets and dressed Li^{q+} ($q = 1, 2$) projectiles, *J. Phys. B: At., Mol. Opt. Phys.* **47**, 155204 (2014).
- [45] M. Kuzel, L. Sarkadi, J. Pálinkás, P. A. Závodszy, R. Maier, D. Berényi, and K. O. Groeneveld, Observation of enhanced emission of cusp electrons at impact of excited metastable neutral He projectiles, *Phys. Rev. A* **48**, R1745 (1993).